



Title	Electro-optics of blue phase liquid crystal in field-perpendicular direction
Author(s)	Zhang, Yuxian; Yoshida, Hiroyuki; Wang, Qiong Hua et al.
Citation	Applied Physics Letters. 2023, 122(16), p. 161107
Version Type	AM
URL	https://hdl.handle.net/11094/91413
rights	This article may be downloaded for personal use only. Any other use requires prior permission of the author and AIP Publishing. and may be found at https://doi.org/10.1063/5.0142383 .
Note	

The University of Osaka Institutional Knowledge Archive : OUKA

<https://ir.library.osaka-u.ac.jp/>

The University of Osaka

Electro-optics of blue phase liquid crystal in field-perpendicular direction

Yuxian Zhang,¹ Hiroyuki Yoshida,^{2, a)} Qiong-Hua Wang^{1, b)} and Masanori Ozaki²

AFFILIATIONS

1. School of Instrumentation and Optoelectronic Engineering, Beihang University, Beijing 100191, China.

2. Division of Electrical, Electronic and Infocommunications Engineering, Graduate School of Engineering, Osaka University, 2-1 Yamada-oka, Suita, Osaka 565-0871, Japan.

Authors to whom correspondence should be addressed:

a) yoshida@eei.eng.osaka-u.ac.jp

b) qionghua@buaa.edu.cn

This is the author's peer reviewed, accepted manuscript. However, the online version of record will be different from this version once it has been copyedited and typeset.

PLEASE CITE THIS ARTICLE AS DOI: 10.1063/5.0142383

1 **ABSTRACT**

2 The electro-optic effect is the working principle of blue phase (BP) liquid crystals, and it describes
3 the relationship between the field-induced birefringence of BPs and the field strength. Due to the
4 electrostriction of BP crystals under the electric field, a tetragonal crystal is usually obtained when the
5 field is applied along one of the two-fold axes of a BP crystal, leading to the optical biaxiality under
6 electric field. Such field-induced optical biaxiality of BPs has been predicted and observed, but its
7 dependence on the field strength has not been investigated. In this research, we analyze the electro-optics
8 in the field-perpendicular direction by measuring the birefringence in highly ordered BP I₍₁₁₀₎ crystals
9 perpendicular to the electric field. Results reveal that BP I crystals in the field-perpendicular direction
10 show an electro-optic coefficient of the order of 10^{-10} m/V² that may result from the large lattice
11 deformation of BP crystals perpendicular to the electric field. Our research provides important
12 experimental evidence for the tensorial properties of BP Kerr effect and may have important implications
13 on the engineering of BP electro-optical devices in practical applications.

Blue phases (BPs) are observed in highly chiral cholesteric liquid crystals (LCs), exhibiting periodic superstructures with the lattice constant of 100~300 nm.^{1,2} Due to the cubic symmetry, BPs are considered to be optical isotropic at zero field intensity. In the presence of electric field, the deflection of LC director leads to a variation of the refractive index in the field direction relative to its orthogonal directions, resulting in the field-induced birefringence.^{3,4} For moderate field intensities, the induced birefringence is proportional to the square of field intensity, as given by the well-known Kerr Effect,^{5,6}

$$\Delta n = \lambda K E^2 \quad (1)$$

where λ is the wavelength of probe light, K is the electro-optic coefficient (also known as the Kerr coefficient) and E is the intensity of applied electric field. Eq. (1) gives the form of quadratic electro-optic effect that describes the birefringence induced in BPs between the field direction and the field-perpendicular directions, resulting from the local reorientation of LC director that corresponds to the response time of sub-milliseconds. In practical operations, the mathematical model of BP Kerr effect has been extended or modified to suit a larger range of field strength or wavelength.^{7,8} However, in the above expressions about the BP electro-optics, the electro-optic coefficient (K) is treated as a scalar, without considering the field-induced biaxiality.^{9,10}

Optical biaxiality in BPs is mainly caused by the electrostriction in which the BP crystal is deformed in three dimensions, which corresponds to a response time of a few milliseconds and is generally negligible relative to the uniaxial component.¹¹ However, the biaxial effect in BPs is not insignificant when the symmetry elements are taken into account. For example, optically biaxial crystals are usually obtained upon an electric field along a two-fold axis of BPs, such as the orthorhombic BP I crystals (F222) under the electric field along [110] axis.¹² Therefore, the electro-optic coefficient of BPs is actually a tensor that relates to the symmetries and depends on which crystal axis the fields are applied, as Eq. (2) shows.^{13,14}

$$\Delta\left(\frac{1}{n^2}\right)_{1,2,3,4,5,6} = \begin{bmatrix} s_{11} & s_{12} & s_{12} & 0 & 0 & 0 \\ s_{12} & s_{11} & s_{12} & 0 & 0 & 0 \\ s_{12} & s_{12} & s_{11} & 0 & 0 & 0 \\ 0 & 0 & 0 & s_{44} & 0 & 0 \\ 0 & 0 & 0 & 0 & s_{44} & 0 \\ 0 & 0 & 0 & 0 & 0 & s_{44} \end{bmatrix} \begin{bmatrix} E_x^2 \\ E_y^2 \\ E_z^2 \\ E_y E_z \\ E_z E_x \\ E_x E_y \end{bmatrix} \quad (2)$$

1 In Eq. (2), Δn_i is the change of refractive index of BPs produced by the electric field E_j ; s_{ij} is a tensor that
2 gives the electro-optical effects. Here in cubic BP I crystals, s_{ij} is composed of only three independent
3 elements (s_{11} , s_{12} and s_{44}) because of the 432 symmetry of BP I.¹⁴ Up to date, the tensorial property of
4 Kerr effect has been reported in BPs,¹⁵⁻¹⁷ but the electro-optics in the field-perpendicular directions have
5 not been measured or quantitatively analyzed. Since it has been revealed that BP monodomains showed
6 improved electro-optical performance compared with the traditional BP multidomain sample without any
7 alignment control,¹⁸⁻²¹ the electro-optic properties of BPs that relates to the crystallography should be
8 considered. Different from the conventional Kerr effect of BPs that mainly comes from the rearrangement
9 of molecules, in this research, we investigate the electro-optics that results from the lattice deformation,
10 which may provide experimental evidence for the tensorial properties of BP Kerr effect and may have
11 important implications in practical applications.

12 Here we focus on the electro-optics of BPs in the field-perpendicular directions as the BP I crystals
13 are deformed by an electric field. By confining highly ordered BP I₍₁₁₀₎ (the subscript (110) indicates the
14 lattice plane parallel to the cell substrate) crystals in a sandwiched cell and applying an electric field along
15 [110] axis, optical birefringence induced in the field-perpendicular direction ($\Delta n_{E\perp}$) is measured, from
16 which the electro-optic coefficient in the field-perpendicular directions ($K_{E\perp}$) is estimated. We find that
17 the electro-optic coefficient in the field-perpendicular direction could not be ignored in BPs ($K_{E\perp} \approx 10^{-10}$
18 m/V²), which may result from the large lattice deformation perpendicular to the electric field.

19 The BP material is prepared by mixing two kinds of nematic LCs with positive dielectric anisotropy
20 4-cyano-4'-n-pentyl-biphenyl (5CB) and JC-1041XX from JNC Corporation, with a chiral dopant ISO-
21 (6OBA)₂ (synthesized)²² at the weight ratio of 46.75%: 46.75%: 6.5%. Phase sequence of the material is
22 identified to be isotropic (47.6 °C) BP II (46.5 °C) BP I (44.8 °C) Cholesteric in a cooling process. To
23 measure the electro-optics of BPs perpendicular to the electric field, BP I₍₁₁₀₎ crystals are prepared in a
24 parallel alignment (PA) cell, which is made of a pair of ITO-coated glass substrates and the electric field
25 could be applied along the direction vertical to the substrates. In order to prepare BP I₍₁₁₀₎ monodomains,
26 glass substrates are cleaned before used. After spin-coating a photoalignment layer (LIA-03, DIC) on the

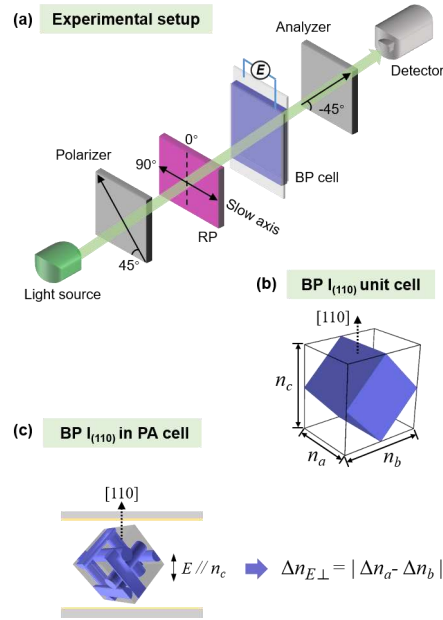
1 substrates and assembling them into a sandwiched cell, uniform alignment is obtained by irradiating the
2 cell with a linearly polarized light of $34 \text{ mW} \cdot \text{cm}^{-2}$ for 60 s.²³ The BP materials are injected into the cell
3 in isotropic phase at 60 °C. By heating the BP cell from cholesteric phase in room temperature to BP II
4 (47.2 °C), and then cooling it to BP I (46.3 °C) at a very slow rate of 0.05 °C/min, BP I₍₁₁₀₎ crystals with
5 highly ordered arrangement are obtained. The optical texture of BPs is observed in a polarized optical
6 microscope (POM, Eclipse LV100-POL, Nikon) and the Kossel diffraction pattern is obtained in the back
7 focal plane of the POM by illuminating a convergent monochromatic light (obtained by a filter of 440 ± 5
8 nm) through the objective lens.

9 During the electro-optical measurement, the BP cell is kept at an invariant temperature on a hotstage
10 (10084L-T96-HS, Linkam). Electric field is applied using a function generator (Agilent, 33210A)
11 equipped with a voltage amplifier (NF Corporation, 4010), with a frequency of 1 kHz between the
12 electrodes. Field intensity is controlled by a computer to increase gradually with an equal gradient
13 ($\Delta E = 0.06 \text{ V}/\mu\text{m}$) and each field intensity is held for 30 s for the optical measurement. The transmission or
14 reflection spectra are measured by a fiber-coupling spectrometer (PMA-11) from Hamamatsu Photonics.

15 FIG. 1a shows the setup for the electro-optical measurement, where a halogen lamp is used as the
16 light source. A full-wave plate of 530 nm is inserted at an angle of 45° with respect to the polarizing axes
17 of the polarizers, working as the uniaxial retardation plate (RP). The retardation of the waveplate is
18 measured in supplementary material (FIG. S1). BP materials confined in a 6.8 μm thick cell is placed
19 between a pair of crossed polarizers and the RP. As an increasing electric field is applied upon the BP cell,
20 transmission spectra are recorded by a detector. In this experiment, the total phase retardation of light
21 comes from the RP and BP sample, and the output light intensity through the system follows Eq. (3),

$$22 \quad I(\lambda) \propto \sin^2 \left[\frac{\Delta S_{RP} + (\Delta n_{E\perp} d)_{BP}}{\lambda} \pi \right] \quad (3)$$

23 in which I is the transmission intensity; λ is the light wavelength; ΔS_{RP} is the light retardation from RP;
24 $\Delta n_{E\perp}$ is the birefringence of BPs perpendicular to the electric field and d is the cell-gap. At the voltage-off
25 state, $(\Delta n_{E\perp} d)_{BP}$ is zero based on the assumption that BPs are optical isotropic, and the light retardation
26 only comes from the RP, leading to the minimum of light intensity $I(\lambda)$ at a certain wavelength (λ_0).



1
2
3
4
5
6

FIG. 1. (a) Experimental setup showing the method to measure the electro-optics of BPs perpendicular to the electric field. (b) Schematic of the BP I lattice in a unit cell and the refractive indices along different crystal axes. (c) Measurement of the BP birefringence induced in the field-normal directions by confining BP I₍₁₁₀₎ crystals in a PA cell.

7 Under an increasing electric field, the transmission wavelength shifts because of the variation of BP
8 birefringence, and the field-induced retardation of BPs is compensated where the transmittance reached
9 the minimum at a certain wavelength λ . This state of minimum transmittance is achieved as soon as the
10 argument of the sine function turns to π . Therefore, by obtaining the wavelength λ at which the
11 transmittance becomes the minimum $I(\lambda)$ under a certain field intensity, $(\Delta n_{E\perp}d)_{BP}$ is yield by deducting
12 $\lambda\omega$. Further, the electro-optic coefficient of BPs perpendicular to the electric field ($K_{E\perp}$) will be obtained
13 by analyzing the relationship of $\Delta n_{E\perp}$ and field strength. Under an increasing electric field, the refractive
14 index of BPs varies along different crystal axes, as shown in FIG. 1b. The working principle of measuring

the electro-optics in the field-perpendicular direction is that in PA cells, BP I crystals orient with their $[110]$ axes along the field direction and the birefringence is measured between the principal axes of BP I crystals perpendicular to the electric field (FIG. 1c). The sign of the BP birefringence can be inferred by noticing whether the direction of interest is parallel or perpendicular to the slow axis for cancellation.

The electro-optics in the field-perpendicular directions is measured by applying an electric field upon the BP $I_{(110)}$ crystals in a PA cell (cell-gap=6.8 μm). FIG. 2a-b show the optical texture and Kossel diffraction pattern of the BP $I_{(110)}$ sample, in which the uniform color and two-fold diffraction pattern confirm the ordered alignment of BP I crystals with their (110) plane parallel to the substrates. We try to measure the birefringence induced along the orthogonal directions of BP I crystals perpendicular to the field, and the cell is rotated to make two principal axes respectively parallel to the RP axes (fast axis or slow axis), as shown in FIG. 2c-d. In our measurement, $[001]$ axis is parallel to the slow axis of RP and in this case, the setup measures the electro-optics induced between $[001]$ and $[\bar{1}10]$ axes of the BP I crystals, which are orthogonal to each other in the field-perpendicular directions.

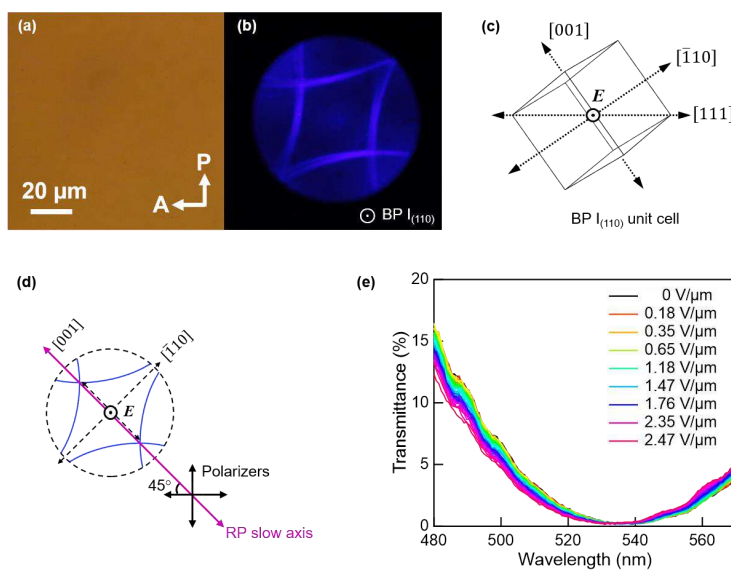


FIG. 2. Measurement of BP electro-optics in the field-perpendicular direction: (a-b) POM images

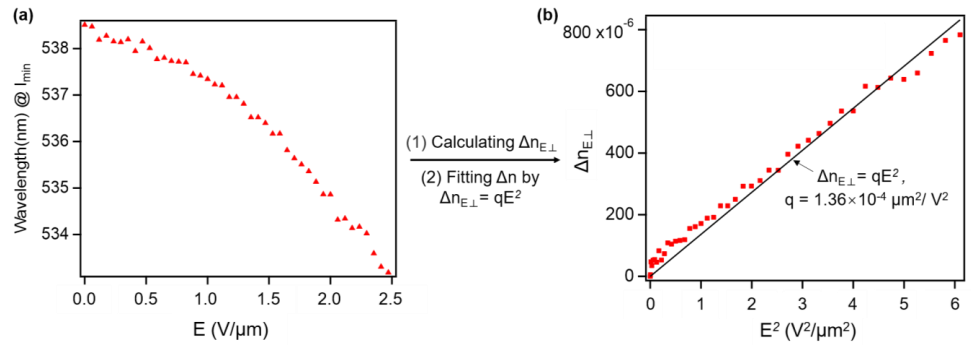
1 and Kossel diffraction pattern of the BP $I_{(110)}$ sample at zero field intensity. (c) Schematic of a BP $I_{(110)}$
 2 unit cell, showing the azimuthal lattice orientation in FIG. 2b and the direction of electric field. (d)
 3 Configuration of our measurement, showing the orientations of BP $I_{(110)}$ crystal axes, RP and polarizers.
 4 (e) Transmission spectra of the BP $I_{(110)}$ sample under electric field. The texture, Kossel diffraction and
 5 transmission spectra are measured by the in-situ measurements on the POM using different objective
 6 lens, and a comparison of the measurement area is shown in the supplementary material (FIG. S2).
 7

8 As a gradually increasing electric field is applied upon the PA cell, transmittance spectra are recorded
 9 at each field intensity. FIG. 2e plots the field dependence of the transmittance of the BP $I_{(110)}$ sample in a
 10 PA cell, where the trough around 540 nm corresponds to the interference minimum generated by the
 11 birefringence perpendicular to the electric field. Since the BP I crystal has its [001] axis orienting along
 12 the slow axis of RP (FIG. 2d), the optical retardation should decrease by applying an increasing field. In
 13 FIG. 2e, we observe a gradual blue shift of the transmission spectra under the increasing field intensity,
 14 corresponding to a decrease of the birefringence $(\Delta n_\lambda)_{BP}$, which is consistent with what is expected by our
 15 experimental configuration.

16 In order to analyze the field-induced birefringence in BPs that relates to the crystal structure, only
 17 the phase transition from cubic ($I4_132$) to tetragonal ($I4_122$) BPs are interested,^{24, 25} which limits the field
 18 intensity to $E \leq 2.5$ V/ μ m in this experiment.^{26, 27} Firstly, by analyzing the small shifts between the troughs
 19 of transmission spectrum, the wavelength at which the transmittance becomes minimum is shown in FIG.
 20 3a, which is found to decrease in a parabolic trend versus the increasing field strength. The minimum
 21 transmittance at varied field intensities is about 0.2% (FIG. S3 in supplementary material).

22 The birefringence of BPs in the field-perpendicular direction $(\Delta n_{E\perp})$ at each field intensity is obtained
 23 by dividing the shift of the transmission minimum by cell-gap. FIG. 3b plots the values of $\Delta n_{E\perp}$ versus
 24 the square of field intensities (E^2), in which we find a linear relationship between $\Delta n_{E\perp}$ and E^2 , indicating
 25 that the electro-optics in the field-perpendicular direction is of a Kerr type, similar with that in Eq. (1). To
 26 quantify the relationship between $\Delta n_{E\perp}$ and the field strength, a linearly positive proportional function of

1 $\Delta n_{E\perp} = qE^2$ is used to fit the experimental data. Further, by dividing the slope ($q=1.36\times 10^{-4} \mu\text{m}^2/\text{V}^2$) of the
 2 fitting line by the wavelength of 540 nm, the electro-optic coefficient induced perpendicular to the field is
 3 evaluated to be $K_{E\perp}=2.5\times 10^{-10} \text{ m/V}^2$.



4
 5 **FIG. 3.** (a) A scatter diagram showing the wavelength at which the transmittance becomes
 6 minimum of the BP I₍₁₁₀₎ sample under varied field intensities in the PA cell.
 7 (b) A scatter diagram of $\Delta n_{E\perp}$ against E^2 , and the linearly fitting by $\Delta n_{E\perp} = qE^2$.
 8

9 It is known that BP materials typically have a Kerr coefficient ranging from 10^{-10} to 10^{-9} m/V^2 , and
 10 here the electro-optic coefficient induced perpendicular to the field direction, which has been neglected in
 11 most studies, is measured to be within this range. Previous works have reported the birefringence in BP I
 12 under weak field strength,^{12,28} which confirmed the effect of BP electrostriction on its electro-optics. In
 13 our research, the birefringence of BPs induced in the field-perpendicular direction, i.e., the optical
 14 biaxiality, may come from the same origins. It is well known that in atomic crystals, the type of optical
 15 anisotropy (uniaxial or biaxial) is related to crystal symmetry, and we believe that in a similar manner, the
 16 optical anisotropy in BPs is attributed to the cubic-to-orthorhombic deformation of the BP crystals under
 17 an electric field.

18 To analyze the lattice deformation of BP I crystals during the electrostriction, in-situ measurements
 19 are performed by measuring the reflection spectrum and Kossel diffraction under the electric field. As FIG.

4 shows, the redshift of Bragg peak and the symmetry transitions in Kossel diffraction patterns indicate that the BP I lattice undergoes considerable lattice deformation upon electrostriction, including both an elongation along the field (FIG. 4a) and a shrinkage perpendicular to the field (FIG. 4b).

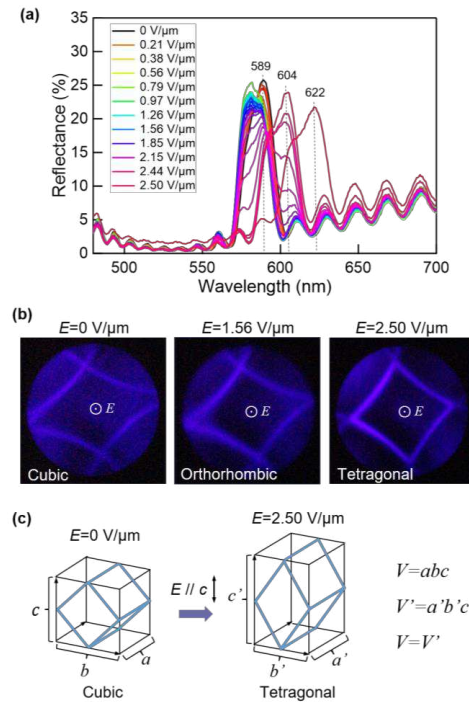


FIG. 4. In-situ measurements of the BP lattice deformation under varied field intensities: (a) reflection spectra, in which the central wavelengths are: $\lambda=589$ nm at $E=0$ V/ μ m; $\lambda=604$ nm at $E=2.44$ V/ μ m; $\lambda=622$ nm at $E=2.50$ V/ μ m. (b) Kossel diffraction patterns, respectively indicating the cubic ($I4_132$), orthorhombic ($F222$) and tetragonal ($F4_122$) symmetries of BP I crystals. (c) An illustration showing the volume-preserved lattice deformation of a BP I unit cell from cubic to tetragonal phase.

Based on the assumption of volume conservation of the BP unit cell under a weak field strength,^{29, 30} one can estimate the BP lattice constants both along and perpendicular to the field. FIG. 4c shows the

1 volume-preserved lattice deformation of a BP I unit cell from cubic phase to tetragonal phase, in which c
2 is the lattice constant along the electric field and a, b are the lattice constants perpendicular to the electric
3 field. Further, by use of the cubic and tetragonal configurations of BP I, we calculate the lattice-constant
4 values respectively at $E=0$ V/ μm and $E=2.50$ V/ μm , as shown in TABLE 1. Therefore, during the field-
5 induced phase transitions from cubic to tetragonal phase, BP I crystals undergo a larger lattice deformation
6 perpendicular to the electric field ($\Delta a=41$ nm, $\Delta b=68$ nm) than that along the electric field ($\Delta c=21$ nm),²⁷
7 which may lead to the large electro-optic coefficient perpendicular to the electric field ($K_{E\perp}$).

8
9 **TABLE 1.** Lattice constants of the BP I₍₁₁₀₎ crystals respectively at $E=0$ V/ μm and $E=2.50$ V/ μm (more
10 details about the calculation are given in the Part II of supplementary material)

Field Intensity	Symmetry	a	b	c
0 V/ μm	Cubic (I4 ₁ 32)	264 nm	373 nm	373 nm
2.50 V/ μm	Tetragonal (F4 ₁ 22)	305 nm	305 nm	394 nm

11
12 In addition, the electro-optics of BP I₍₁₁₀₎ crystals confined in higher cell-gaps (9.9 μm and 14.8 μm)
13 are measured in the field-perpendicular direction (FIG. S5 in supplementary material), in which we also
14 observe a gradual increase of $\Delta n_{E\perp}$ upon the increase of E^2 , as that in the 6.8 μm cell. These results
15 indicate that the large optical anisotropy of BPs induced perpendicular to the electric field is not caused
16 by the confinement of thin cell-gap, but may result from the lattice deformation in the field-perpendicular
17 direction. However, a nonlinear relationship between $\Delta n_{E\perp}$ and E^2 is obtained for higher cell-gaps, which
18 may require further investigation.

19 In conclusion, the electro-optics in the field- perpendicular direction is investigated by measuring the
20 birefringence induced perpendicular to the electric field. Similar to the conventional Kerr effect under
21 moderate fields, a quadratic relationship between the induced birefringence and squared field intensities
22 is observed. By fitting the experimental data using a positive proportional function, we calculate that the
23 electro-optic coefficient in the field-perpendicular direction is in the order of 10^{-10} m/V². Our work

1 experimentally confirms the optical biaxiality in BPs, which provides a fundamental insight into the
2 tensorial properties of BP electro-optic effect. The electro-optics of BPs that relates to crystallography
3 may have important implications on the engineering of BP devices in practical applications.

4
5 See the supplementary material for (I) Details about the electro-optical measurements; (II)
6 Calculation of the lattice constants of BP I; (III) Electro-optics of BP I₍₁₁₀₎ crystals in thick cells.

7 Y. Zhang and Q.-H. Wang acknowledge the support from the National Natural Science Foundation
8 of China (62005008, 61927809) and Shenzhen Science and Technology Innovation Commission
9 (JCYJ20220818100413030). H. Y. acknowledges funding by the National Science Centre, Poland under
10 the OPUS call in the Weave program (UMO-2021/43/I/ST5/02632), the Czech Science Foundation
11 (Project No. 22-42944L), JSPS KAKENHI (19H02581) and MEXT Leading Initiative for Excellent
12 Young Researchers Grant Number JPMXS0320200123.

AUTHOR DECLARATIONS

Conflict of Interest

The authors have no conflicts to disclose.

DATA AVAILABILITY

The data that support the findings of this study are available from the corresponding author upon reasonable request.

REFERENCES

- ¹H. Stegemeyer, T. H. Blümel, K. Hiltrop, H. Onusseit and F. Porsch, *Liq. Cryst.* **1**, 3-28 (2007).
- ²D. C. Wright and N. D. Mermin, *Rev. Mod. Phys.* **61**, 385-432 (1989).
- ³F. Porsch and H. Stegemeyer, *Liq. Cryst.* **2**, 395-399 (2007).
- ⁴Y. Hisakado, H. Kikuchi, T. Nagamura and T. Kajiyama, *Adv. Mater.* **17**, 96-98 (2005).
- ⁵J. Kerr, *Philos. Mag.* **50**, 337-348 (1875).
- ⁶P. R. Gerber, *Mol. Cryst. Liq. Cryst.* **116**, 197-206 (1985).

This is the author's peer reviewed, accepted manuscript. However, the online version of record will be different from this version once it has been copyedited and typeset.

PLEASE CITE THIS ARTICLE AS DOI: 10.1063/5.0142383

- ⁷J. Yan, H.-C. Cheng, S. Gauza, Y. Li, M. Jiao, L. Rao and S.-T. Wu, Appl. Phys. Lett. **96**, 071105 (2010).
- ⁸B. Atorf, H. Rasouli, G. Nordendorf, D. Wilkes and H. Kitzerow, Appl. Phys. Lett. **108**, 081107 (2016).
- ⁹V. E. Dmitrienko, Liq. Cryst. **5**, 847-851 (1989).
- ¹⁰H. S. Kitzerow, Mol. Cryst. Liq. Cryst. **202**, 51-83 (1991).
- ¹¹H. Choi, H. Higuchi and H. Kikuchi, Soft Matter **7**, 4252-4256 (2011).
- ¹²F. Porch, H. Stegemeyer and K. Hiltrop, Z. Naturforsch **39a**, 475-480 (1984).
- ¹³M. Born, E. Wolf, Principles of optics : electromagnetic theory of propagation, interference, and diffraction of light, Pergamon Press, London (1964).
- ¹⁴J. F. Nye, Physical properties of crystals : their representation by tensors and matrices, Clarendon Press, Oxford (1984).
- ¹⁵Y. Kawata, H. Yoshida, S. Tanaka, A. Konkanok, M. Ozaki and H. Kikuchi, Phys. Rev. E **91**, 022503 (2015).
- ¹⁶H.-S. Kitzerow, Ferroelectrics **395**, 66-85 (2010).
- ¹⁷U. Singh and P. H. Keyes, Liq. Cryst. **8**, 851-860 (1990).
- ¹⁸P. Nayek, H. Jeong, H. R. Park, S.-W. Kang, S. H. Lee, H. S. Park, H. J. Lee and H. S. Kim, Appl. Phys. Express **5**, 051701 (2012).
- ¹⁹Y. Chen and S.-T. Wu, Appl. Phys. Lett. **102**, 171110 (2013).
- ²⁰E. Oton, E. Netter, T. Nakano, Y. D.-Katayama and F. Inoue, Sci. Rep. **7**, 44575 (2017).
- ²¹C.-W. Chen, C.-T. Hou, C.-C. Li, H.-C. Jau, C.-T. Wang, C.-L. Hong, D.-Y. Guo, C.-Y. Wang, S.-P. Chiang, T. J. Bunning, I.-C. Khoo and T.-H. Lin, Nat. Commun. **8**, 1-8 (2017).
- ²²O. Parry, P. Nolan, L. Farrand and A. L. May, WO9800428 (1998).
- ²³M. Takahashi, T. Ohkawa, H. Yoshida, J.-i. Fukuda, H. Kikuchi and M. Ozaki, J. Phys. D: Appl. Phys. **51**, 104003 (2018).
- ²⁴G. P. Alexander and D. Marenduzzo, EPL-Europhys. Lett. **81**, 66004 (2008).
- ²⁵H. Yoshida, S. Yabu, H. Tone, H. Kikuchi and M. Ozaki, Appl. Phys. Express **6**, 062603 (2013).
- ²⁶Y. Zhang, H. Yoshida, S. Cho, J.-i. Fukuda and M. Ozaki, ACS Appl. Mater. Inter. **13**, 36130-36137

This is the author's peer reviewed, accepted manuscript. However, the online version of record will be different from this version once it has been copyedited and typeset.

PLEASE CITE THIS ARTICLE AS DOI: 10.1063/5.0142383

(2021).

²⁷Y. Zhang, H. Yoshida, F. Chu, Y. Q. Guo, Z. Yang, M. Ozaki and Q. H. Wang, *Soft Matter* **18**, 3328-3334

(2022).

²⁸H. Yoshida, S. Yabu, H. Tone, Y. Kawata, H. Kikuchi and M. Ozaki, *Opt. Mater. Express* **4**, 960-968

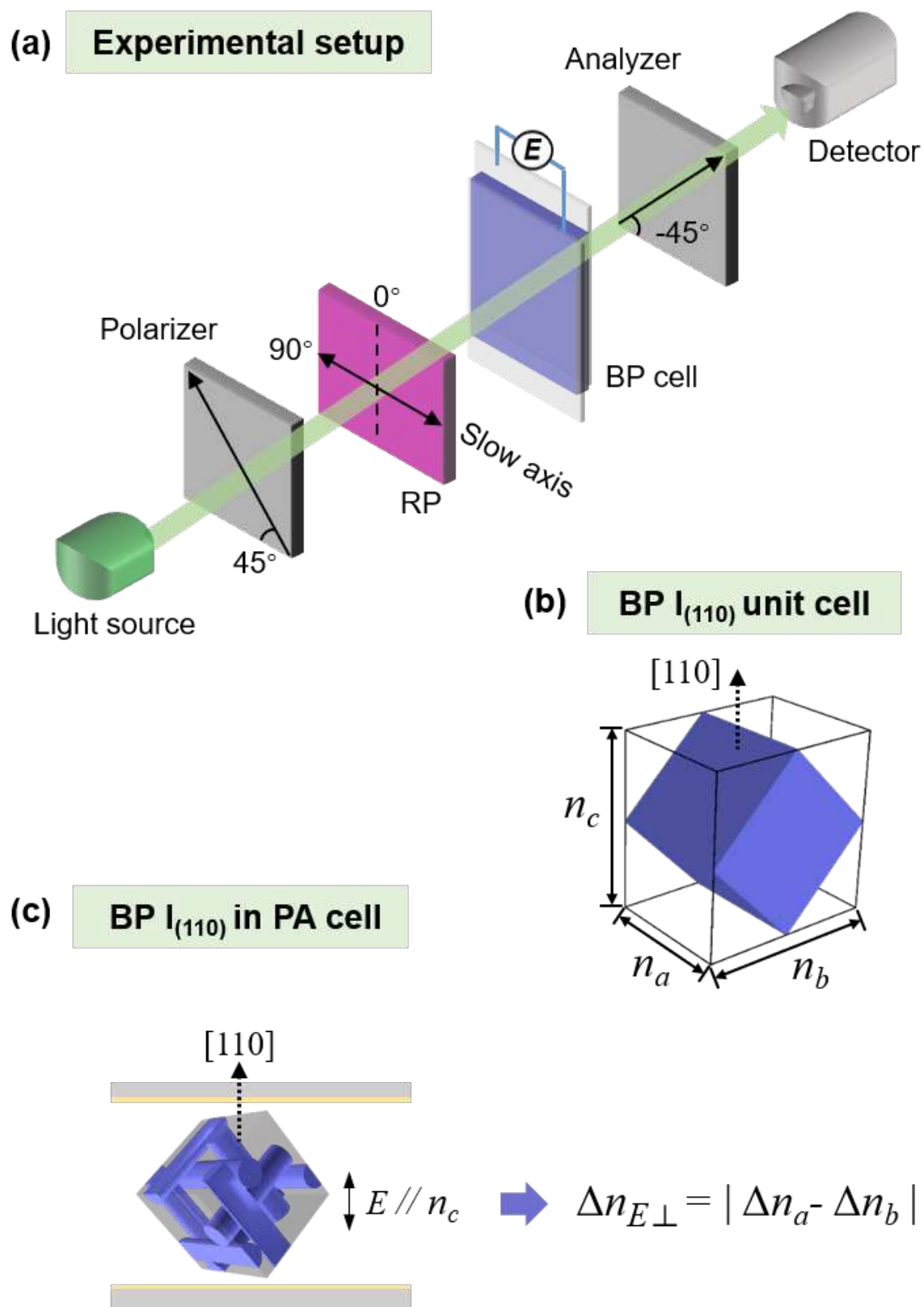
(2014).

²⁹G. Heppke, B. Jérôme, H. S. Kitzerow and P. Pieranski, *J. Phys. (France)* **50**, 549-562 (1989).

³⁰J.-i. Fukuda, M. Yoneya and H. Yokoyama, *Phys. Rev. E* **80**, 031706 (2009).

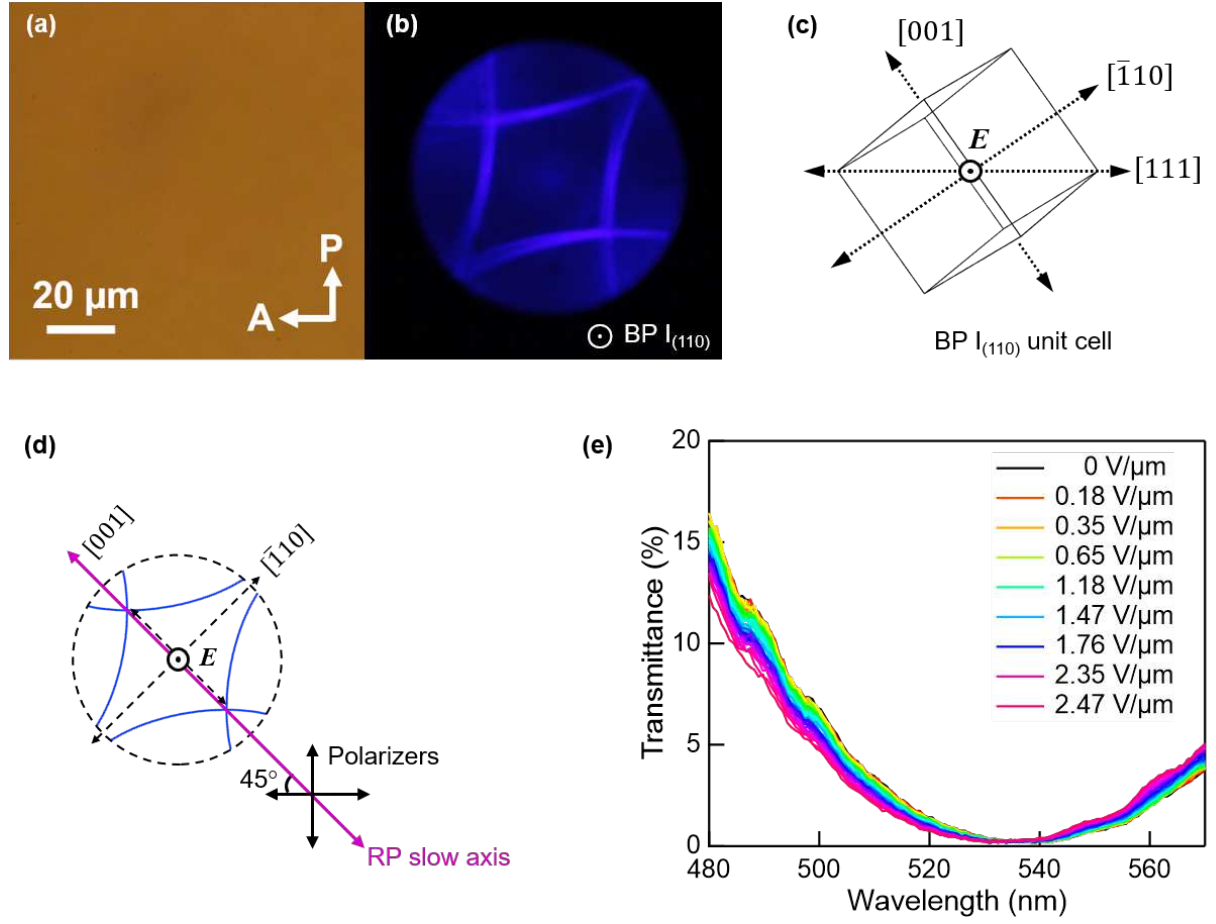
This is the author's peer reviewed, accepted manuscript. However, the online version of record will be different from this version once it has been copyedited and typeset.

PLEASE CITE THIS ARTICLE AS DOI: 10.1063/5.0142383



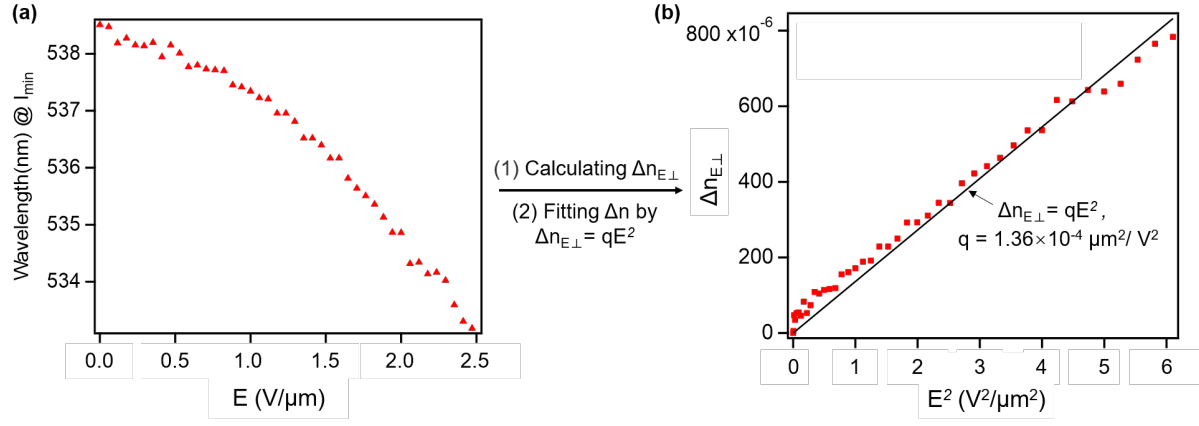
This is the author's peer reviewed, accepted manuscript. However, the online version of record will be different from this version once it has been copyedited and typeset.

PLEASE CITE THIS ARTICLE AS DOI: 10.1063/5.0142383



This is the author's peer reviewed, accepted manuscript. However, the online version of record will be different from this version once it has been copyedited and typeset.

PLEASE CITE THIS ARTICLE AS DOI: 10.1063/5.0142383



This is the author's peer reviewed, accepted manuscript. However, the online version of record will be different from this version once it has been copyedited and typeset.

PLEASE CITE THIS ARTICLE AS DOI: 10.1063/5.0142383

